Trapping and Beamloading in hybrid Plasma Wakefield Accelerator schemes

Alexander Knetsch

November 29, 2016

CONTENTS

1. THEORY

1.1 Plasma physics

There are several definitions of a plasma, but one of the most appealing one that we will follow in this work can be found in the classic textbook by Francis F. Chen: "A plasma is a quasineutral gas of charged and neutral particles which exhibits collective behavior" [1]. Regarding the gas types we will conveniently assume them to be electrons, ions and neutral atoms and comment that other particles as well can fit the definition of a plasma, but such exotic compositions are beyond the scope of this work. As plasmas are electromagnetically interacting a common and very useful way to describe it on a fundamental level is with the help of the Maxwell equation.

$$\vec{\nabla}\vec{E} = \frac{\rho}{\epsilon_0},\ \vec{\nabla}\vec{B} = 0\,\vec{\nabla}\times\vec{E} = -\frac{\partial\vec{B}}{\partial t},\ \vec{\nabla}\times\vec{B} = \mu_0\vec{j} + \mu_0\epsilon_0\frac{\partial\vec{E}}{\partial t}. \tag{1.1}$$

$\vec{E}$ and $\vec{B}$ are the electric and magnetic field and $\vec{j}$ and ρ is the current density and charge density. ϵ_0 and μ_0 are the vacuum dielectric constant and the vacuum permeability. They are connected with the vacuum speed of light c through the relation $c = 1/\sqrt{\mu_0\epsilon_0}$ In a fluid description it makes also sense to assume that no particles are created or destroyed which is the origin of the continuity equation

$$\frac{\partial\rho}{\partial t} + \vec{\nabla}(\rho\vec{v}) = 0. \tag{1.2}$$

Plasma frequency

Electrons and ions in a plasma can be described as two fluids, each following the fluid dynamics and interacting via electrodynamics and collisions.

A displacement of the electron fluid with respect to the ion fluid leads to strong electric fields, acting upon both as a restoring force, but as $m_\mathrm{i} >> m_\mathrm{e}$, the electron response is much quicker which is why these kind of plasma oscillations are dominated by the electrons, while the ions can be considered inert.

Starting from equation (1.9) with the relation of the electric field and its potential being $\vec{E} = -\nabla\Phi$

$$\epsilon_0\nabla\vec{E} = q_\mathrm{e}(n_\mathrm{i} - n_\mathrm{e}) \tag{1.3}$$

becomes for small perturbations $n' = n_\mathrm{e} + \delta n$

$$\epsilon_0\nabla\vec{E} = q_\mathrm{e}\delta n). \tag{1.4}$$

The solution to this differential equation is a harmonic density oscillation

$$n(x,t) = \delta n\exp(i(kx - \omega_\mathrm{p}t)). \tag{1.5}$$

The characteristic frequency of this oscillation

$$\omega_\mathrm{p} = \sqrt{\frac{n_\mathrm{e} q_\mathrm{e}^2}{\epsilon_0 m_\mathrm{e}}} \tag{1.6}$$

is called the *Plasma frequency* and is one of the most important parameters in plasma physics. In the field of PWFA it is convenient to also consider the wavelength associated with the plasma oscillations, the *Plasma wavelength*

$$\lambda_\mathrm{p} = 2\pi \frac{\omega_\mathrm{p}}{c}. \tag{1.7}$$

Typical values for example for a plasma density $n_\mathrm{e} = 1 \times 10^{17}\mathrm{cm}^{-3}$ are

$$\omega_\mathrm{p} \approx 56400\sqrt{n_\mathrm{e}[\mathrm{cm}^{-3}]} \approx 1.8 \times 10^{18}\ 1/s$$
$$\lambda_\mathrm{p} \approx 105.6/\sqrt{n_\mathrm{e}[10^{17}\mathrm{cm}^{-3}]}[\mu\mathrm{m}] = 105.6\ \mu\mathrm{m}.$$

Debye Shielding

The concept of *quasi-neutrality* roots in the shielding behavior of the ions and electrons of charges inside the plasma. A positive net charge e.g. originating from a difference in ion density n_i and electron density n_e at a temperature T would attract electrons and lead to an electron distribution

$$f(u) \propto \exp(-\frac{1}{2} m_\mathrm{e} v^2 + q_\mathrm{e}/(k_\mathrm{B}T)). \tag{1.8}$$

With the Poisson Equation

$$\epsilon_0 \frac{d^2\Phi}{dx^2} = -q_\mathrm{e}(n_\mathrm{e} - n_\mathrm{i}) \tag{1.9}$$
$$= q_\mathrm{e} n_\mathrm{e}(\exp(q_\mathrm{e}\Phi/(k_\mathrm{B}T)) - 1) \tag{1.10}$$
$$\approx q_\mathrm{e} n_\mathrm{e}(q_\mathrm{e}\Phi/(k_\mathrm{B}T) + ...) \tag{1.11}$$

we can now derive the potential in the plasma

$$\Phi = \Phi_0 \exp(-|x|/\lambda_\mathrm{D}) \tag{1.12}$$

with the information about the range of the shielded Coulomb field embedded in the Debye Radius

$$\lambda_\mathrm{D} = \sqrt{\frac{\epsilon_0 k_\mathrm{B} T}{n_\mathrm{e} q_\mathrm{e}^2}}. \tag{1.13}$$

We can see that a plasma with an edge length $L >> \lambda_\mathrm{D}$ would have its Coulomb fields shielded and appear to an outside observer to be charge-neutral.

1.1.1 electromagnetic waves in plasmas

It is worth noting that the Debye Shielding assumes a thermalized plasma and is not the right idea of a plasma reaction to a rapid change in charge on a femtosecond timescale. The more appropriate figure of merit is to look directly at the propagation of electromagnetic waves in plasma which we will deduct now following [2].

The electromagnetic wave propagation needs to be calculated by applying the Maxwell equations 1.1 so that one gets the differenctial equation.

$$\vec{\nabla} \times \vec{\nabla} \times \vec{E} + c^{-2} \frac{\partial^2 \vec{E}}{\partial t^2} = -\frac{1}{\epsilon_0 c^2} \frac{\partial \vec{j}}{\partial t} \tag{1.14}$$

In plasma the current density is not 0, but only electronic flow velocity $\vec{v_e}$ needs to be taken into account for the high frequencies we are considering in this work so that

$$\vec{j} = -q_e n_e \vec{v_e} \tag{1.15}$$

Equation (1.14) can be solved with an exponential Ansatz for a linear wave

$$\vec{E} = E_0 e^{ikx - i\omega t}) \tag{1.16}$$

so that equation (1.14) becomes

$$\nabla \times \nabla \times \vec{E} - k^2 \eta^2 \vec{E} = \frac{v_g v_{ph}}{c^2} \tag{1.17}$$

with an index of refraction in an absorption-free plasma

$$\eta = \sqrt{1 - \frac{\omega_p^2}{\omega^2}}. \tag{1.18}$$

Equation (1.18) can be interpreted as a criterion for the propagation. For $\omega_p > \omega$ η becomes imaginary which is physically equivalent to a reflection of the wave.

The measure of the depth of intrusion is the skin depth

$$k_p^{-1} = \frac{c}{\sqrt{\omega_p^2 - \omega^2}} \overset{\omega_p \gg \omega}{=} \frac{c}{\omega_p} \tag{1.19}$$

Ergo for the reflection to transparency transitions i.e. at $\omega_p = \omega$ a so called critical plasma density

$$n_{crtit.} = \frac{\epsilon_0 m_e \omega^2}{q_e^2} \tag{1.20}$$

can be defined.

In this work the propagation of several fs short laser pulses with a central wavelength of $\lambda = 800$ nm are going to be looked at. The reason is that experimentally these are the typical parameters for a Titan-Saphire (Ti:Sa) laser system which is the most common one.

For such a laser system the critical density in equation (1.20) is $n_{crit.} = 1.7 \times 10^{21}$ cm^{-3}. As the electron densities essential to the scope of this work are not going to exceed 1×10^{19} cm^{-3}, we can for the rest of this text safely assume that the plasma is opaque for laser light.

1.1.2 Underdense ionization with ultrashort laser pulses

Subpicosecond laser pulses, when equipped with sufficnent intensity, can be used to easily ionize a gas to a plasma. This can be divided in three different regimes, the single-or multiphoton ionization (MPI), the tunnel ionization (TI) and the Barrier suppression ionization (BSI). Multiphoton ionization describes the absorption of one or several photons by a bound electron with the effect that this electron is released into the continuum. In that sense MPI is necessarily an AC effect, as several laser oscillations need to act upon the electron. TI and BSI on the other hand describe an ionization that occurs due to the deformation of the ion potential, which means that the electron is ionized on a time scale on which the laser field can be assumed to be constant, i.e. a DC effect. A handy parameter to distiguish between the regime of multi-photon and tunneling ionization is The Keldysh parameter

$$\gamma_{\mathrm{K}} = \sqrt{\frac{\xi_{\mathrm{ion}}}{2U_p}}, \tag{1.21}$$

A measure of the amount of laser oscillations the electron endures until its ionization that compares the binding energy ξ_{ion} of an electron in an atomic potential to the ponderomotive energy $U_{\mathrm{p}} = \frac{q_{\mathrm{e}}^2 E^2}{4 m_{\mathrm{e}} \omega_{\mathrm{L}}}$ carried out by the laser pulse.

For a Keldysh parameter $\gamma_{\mathrm{K}} < 1$ tunnelling ionization is dominanting and for $\gamma_{\mathrm{K}} > 1$ MPI.

In this work we will work with laser intensities up to $1 \times 10^{16} W/cm^{-2}$ which corresponds to a $\gamma_{\mathrm{K}} < 1$ regime.

Tunneling Ionization can be well decribed with the Ammosov-Delone-Krainov (ADK) model.

In [3] they have extended the tunnel ionization probability of electrons in a hydrogen atom to arbitrary atoms. For example for atoms with orbital quantum number $n* >> 1$ and l and its projection m the tunneling ionization probability for an electron at a binding energy ξ_{ion} being excited by a laser with peak electric field E is

$$w = C_{n*l*}^2 \Big(\frac{3E}{\pi E_0}\Big) \xi_{\mathrm{ion}} \frac{(2l+1)(l+|m|))!}{2^{|m|}|m|!(l-|m|)!} \Big(\frac{2E_0}{E}\Big)^{2n*-|m|-1}. \tag{1.22}$$

$n* = Z/\sqrt{2E}$ with the ionization level Z and $E_0 = \sqrt{2E}$. $C_{n*l*} = (\frac{2q_{\mathrm{e}}}{n*})^{n*}/\sqrt{2\pi n*}$.

In [4] Bruhwiler et al. have developed an approximated equation which is optimated for using it in numerical operations such as PIC codes, where the ADK ionization rate is

$$W_{\mathrm{ADK}} = 1.52 \times 10^{15} \frac{4^{n^*_{\mathrm{eff}}} \xi_{\mathrm{ion}}[eV]}{n^*_{\mathrm{eff}} \Gamma(2n^*_{\mathrm{eff}})} \Big(20.5 \frac{\xi_{\mathrm{ion}}^{3/2}[eV]}{E[GV/m]}\Big)^{2n^*_{\mathrm{eff}}-1} \times \exp(-6.83 \frac{\xi_{\mathrm{ion}}^{3/2}[eV]}{E[GV/m]}) \tag{1.23}$$

for an element to the ionization level Z with its ionization energy ξ_{ion}. $n^*_{\mathrm{eff}} \approx 3.69 Z/\xi_{\mathrm{ion}}$ is the effective principal quantum number. A list of ionization energies can be found in [5]. The actual ionization ratio of a gas with plasma density at a given point in space in the lab frame for full ionization n_0 is then obtained by integrating

$$\frac{n_{\mathrm{e}}(t)}{n_0} = 1 - \exp\Big(-\int_{-\infty}^{t} W_{\mathrm{ADK}}(t')dt'\Big). \tag{1.24}$$

As we treat ultrashort pulses, the time scales in which the ionization occurs is comparable to that of the laser pulse rms length τ. We assume e.g. a laser pulse linearly polarized in y. The electric

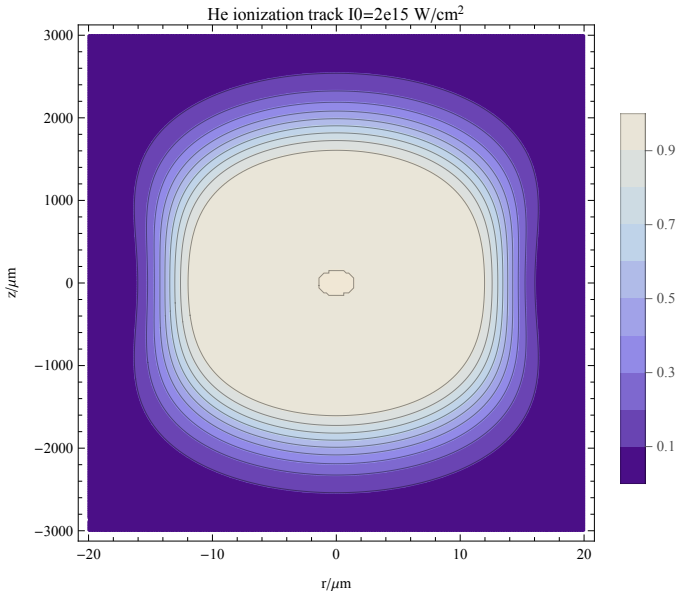

Fig. 1.1: He Ionization ratio by a 1 mJ Gaussian laser pulse with waist $w_0 = 20\ \mu m$ and $\tau = 70$ fs FWHM pulse length

field can be approximated by the envelope of the laser electric field to

$$E_y(t) = E_0 \exp(-\frac{t}{2\tau^2}), \tag{1.25}$$

because the ADK theory averages over DC fields. The complete envelope field distribution of a Gaussian laser in TEM_{00} mode is then

$$E_x(r,z,t) = E_0 \frac{w_0}{w(z)} \exp(-\frac{r^2}{w(z)^2}) \exp(-\frac{t}{2\tau^2}) \tag{1.26}$$

in a cylindrical coordinate system. $w(z) = w_0(1 + (\frac{z}{z_0})^2)^{1/2}$ is the beam waist at longitudinal position z and $z_0 = \pi w_0^2/\lambda$ is the Rayleigh length. Now the complete ADK ionization integral is

$$n_\mathrm{e}(r,z,t) = n_0\Big(1 - \exp\Big(-\int_{-\infty}^{t} W_\mathrm{ADK}(E_x(r,z,t'))dt'\Big)\Big). \tag{1.27}$$

Figure (1.1) shows a plane of the ionization ration n/n_0 of laser-ionized He according to equation (1.27) at $t \gg \tau$. One can see, that sharp density transitions are created transverse to the laser pulse propagation direction. This detail will become important in section (1.8.3) and in the experimental part of the thesis as such sharp transitions are a conventient tool for the injection of electrons in wakes.

1.2 PWFA theory

1.3 The linear regime

Herleitung by esarey [6]

$$E_\xi = 4\pi \int_0^\xi \rho\xi' \cos(k_\mathrm{p}(\xi - \xi'))d\xi \tag{1.28}$$

The transformer ratio $R_\mathrm{trans} = \frac{E^+_\mathrm{max}}{E^-_\mathrm{max}}$ in PWFA is defined as the ratio of the maximum accelerating electric field behind the driving bunch, E^+_max, to the maximum decelerating E^-_max electric field acting upon drive beam electrons. Experimentally the transformer ratio is comparably easy access-able if one assumes the acceleration length for the witness beam and deceleration length for the drive beam to be equal and that the witness beam is in accelerated at the peak accelerating field. Then it can be observed in the electron energy spectrum as the maximum energy gain of the witness beam divided by the maximum energy loss of the drive beam. In that sense the transformer ratio is a measure of efficiency with which the drive electron beam can transfer energy to the witness electron beam. In the linear regime for a Gaussian drive beam In [7] it is calculated and simulated that the transformer in the linear regime, which is otherwise limited to $R_\mathrm{trans} \leq 2$ for a symmetric drive beam current profile [8], can reach up to $R_\mathrm{trans} \approx 6.12$ by applying a triangular shaped drive beam current.

1.4 The blowout regime

Wavebreaking limit:

$$E_\mathrm{WB} = cm_\mathrm{e}\omega_\mathrm{P}/q_\mathrm{e} \simeq 96\sqrt{n_\mathrm{e}(\mathrm{cm}^{-3})} \tag{1.29}$$

original paper: [9]

$$W_r = \partial_r W_z \tag{1.30}$$

1.5 Descriptions for the blowout regime

Lotov, Suk, breakdown of fluid theory Q-tilde and resonant wake excitation.

1.6 Accelerator physics

In the previous chapters we examined the physics of the beam driven plasma wake excitation. The ultimate goal as presented in this work is to advantageously make use of the fields in order to inject and accelerate a high quality secondary electron beam, which is conventionally called the witness beam. If there are no substantial advantages between using the witness over the drive beam for a given application, it might not be worth the effort beyond a scholastic interest. In this section we will explain the basic electron beam behavior in an accelerator and from that determine the most important parameters.

1.6.1 Single particle movement

We start with the

$$\vec{F} = \frac{d\vec{p}}{dt} = q(\vec{E} + \frac{\vec{v}}{c} \times \vec{B}) \tag{1.31}$$

Similar to the assumptions made in par-axial optics the electron can be expected to follow a straight trajectory in the absence of any deflecting or accelerating force and any small change in that trajectory can be expressed in a number of linear changes. As in par-axial optics this gives the possibility to describe the electron beam trajectory with linear transformations, represented by a matrix formalism. This idea can be extrapolated to the entire phase-space information of an electron, so that equation

$$\begin{gathered}\Phi_\mathrm{f} = \hat{R}\Phi_\mathrm{i} \\ \begin{pmatrix} x_\mathrm{f} \\ x'_\mathrm{f} \\ y_\mathrm{f} \\ y'_\mathrm{f} \\ z_\mathrm{f} \\ \delta_\mathrm{f} \end{pmatrix} = \begin{pmatrix} R_{11} & R_{12} & R_{13} & R_{14} & R_{15} & R_{16} \\ R_{21} & R_{22} & R_{23} & R_{24} & R_{25} & R_{26} \\ R_{31} & R_{32} & R_{33} & R_{34} & R_{35} & R_{36} \\ R_{41} & R_{42} & R_{43} & R_{44} & R_{45} & R_{46} \\ R_{51} & R_{52} & R_{53} & R_{54} & R_{55} & R_{56} \\ R_{61} & R_{62} & R_{63} & R_{64} & R_{65} & R_{66} \end{pmatrix} \begin{pmatrix} x_\mathrm{i} \\ x'_\mathrm{i} \\ y_\mathrm{i} \\ y'_\mathrm{i} \\ z_\mathrm{i} \\ \delta_\mathrm{i} \end{pmatrix}\end{gathered} \tag{1.32}$$

describes a complete linear transformation of an electron's phase space vector as a conservative force acts upon it, with the spatial components x, y, z, the transverse momenta $x' = \frac{p_\mathrm{x}}{p_\mathrm{z}}, y' = \frac{p_\mathrm{y}}{p_\mathrm{z}}$ and the deviation $\delta = \frac{\delta p_\mathrm{z}}{p_\mathrm{z}}$ from the design momentum p_z The matrix $\mathbf{R}_{\mathrm{m,n}} = \frac{\delta \Phi_\mathrm{n}}{\delta \Phi_\mathrm{n}}$ is the Jacobian of this transformation and as that it requires $\det(\hat{R}) = 1$.

Wiedemann: [10]

Jamies book: [11]

1.6.2 Liouville Theorem

When now considering an entire bunch of electrons it comes in handy to describe it as a smooth phase space distribution $f(\vec{r}, \vec{p})$, which is conventionally normalized to ensure

$$\int_{-\infty}^{\infty} f(\vec{r}, \vec{p}) d\vec{r} d\vec{p} = 1. \tag{1.33}$$

The Liouville Theorem states that if only conservative forces are applied to the bunch the total phase volume occupied by the distribution stays constant. This is mathematically equivalent to any transformation that maintains condition (1.33), which can be expressed by Jacobian transformations of the kind described by equation (1.32). Of course $\hat{R}$ does not need to act upon the entire 6D-Phase space. In fact it is common to reduce the analysis and describe only changes in the transverse phase space, the so called *trace space*, as the planes are mathematically independent and often beam-optics that only influence one plane such as quadropoles or dipoles are applied.

In order to obtain a measure of the actual phase space volume the statistical moments of the distribution can be determined by evaluating the integral

$$< x^n >= \int_{-\infty}^{\infty} f(\vec{r}, \vec{p}) x^n dx. \tag{1.34}$$

1.6.3 Courant-Snyder coefficients, brightness and emittance

Courant and Snyder with their summary paper [12] have set the standard for defining the phase space volume in the trace space with an ellipse equation for its boundary

$$\gamma < x^2 > +2\alpha < x >< x' > +\beta < x'^2 >= \epsilon. \tag{1.35}$$

$$\alpha = \frac{< x^2 >}{\epsilon}, \gamma = \frac{< x'^2 >}{\epsilon}, \alpha = \frac{< xx' >}{\epsilon} \tag{1.36}$$

are the so called *Courant Snyder parameters* with $x' = \frac{p_\mathrm{x}}{p_\mathrm{z}}$ being the ratio between the transverse momentum p_x and the longitudinal momentmum p_z. The constant of the ellipse ϵ is the trace space emittance. As $f(\vec{r}, \vec{p})$ is considered to be smooth function, it might as well consist of a distribution that only approaches 0 so that it is difficult to draw a absolute volume edge as illustrated in figure (1.2). Because of this and for the sake of simplicity in comparing the value with experimental data, it is useful to work with the rms values. So the *rms trace space emittance* according to [13] is

$$\epsilon_\mathrm{tr,rms} = \sqrt{< x^2 >< x'^2 > - < xx' >^2}. \tag{1.37}$$

This can additionally be normalized to the *normalized rms trace space emittance* into the form

$$\epsilon_\mathrm{n,tr,rms} = \frac{p_\mathrm{z}}{m_\mathrm{e}c}\sqrt{< x^2 >< x'^2 > - < xx' >^2} \tag{1.38}$$

so that its value stays current during acceleration. The emittance is an important value, as it is invariant under conservative transformations and therefore an important figure of merit for electron beam quality in general. Definition (1.38) will mostly be applied in the context of this work. As in the forthcoming parts of this work we will have a look at numerical simulations conducted with particle-in-cell (PIC) Simulations, that handle discrete phase space points as electron beam representation instead od a continuum a discrete emittance expression will be used. For that the electron beam moments are sums in the following form.

$$< x^2 > = \frac{1}{n}\sum_{i=1}^{n} x_i^2 - \frac{1}{n^2}\Big(\sum_{i=1}^{n} x_i\Big)^2 \tag{1.39}$$

$$< x' > = \frac{1}{n}\sum_{i=1}^{n} \Big(\frac{p_{x,i}}{p_{z,i}}\Big)^2 - \frac{1}{n^2}\Big(\sum_{i=1}^{n} \frac{p_{x,i}}{p_{z,i}}\Big)^2 \tag{1.40}$$

$$< xx' > = \Big(\frac{1}{n}\sum_{i=1}^{n} x_i\frac{p_{x,i}}{p_{z,i}} - \frac{1}{n^2}\sum_{i=1}^{n} x_i \sum_{j=1}^{n} \frac{p_{x,i}}{p_{z,j}}\Big)^2 \tag{1.41}$$

1.7 Electron Trapping in plasma accelerators

In order to derive an expression for the trapping condition of a single electron in PWFA, one has to start with the equation of motion for such a single electron.

$$\vec{F} = \frac{d\vec{p}}{dt} = q(\vec{E} + \frac{\vec{v}}{c} \times \vec{B}) \tag{1.42}$$

with the electron charge q electric field $\vec{E}$ and magnetic field $\vec{B}$

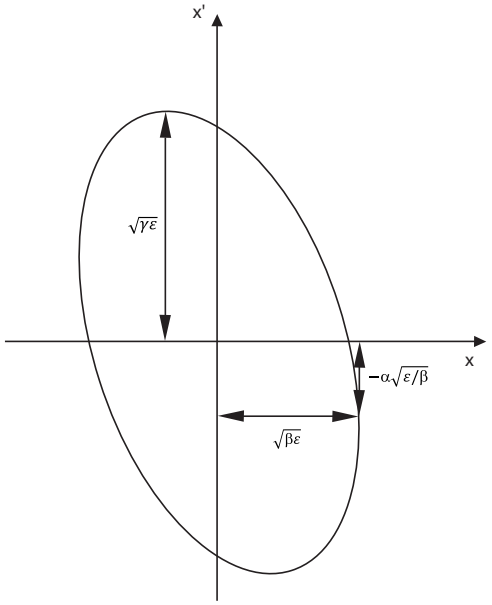

Fig. 1.2: Illustration of the trace space ellipse and its connection to the Courant Snyder coefficients.

This leads to the single particle electron hamiltonian $H = \gamma mc^2 + \Phi$ with the temporal derivative.

$$\frac{dH}{dt} = \frac{d}{dt}(\gamma m_e c^2) + \frac{d}{dt}(q\Phi) \tag{1.43}$$

$$= \vec{v}\frac{d\vec{p}}{dt} + \frac{d}{dt}(q\Phi) \tag{1.44}$$

$$= q\vec{v}(-\nabla\Phi - \frac{\partial\vec{A}}{\partial t}) + \frac{\vec{v}\times\vec{B}}{c} + \frac{d}{dt}(q\Phi) \tag{1.45}$$

$$= q(\frac{d}{dt}\Phi - \vec{v}\vec{\nabla}\Phi - \vec{v}\frac{\partial\vec{A}}{\partial t}) \tag{1.46}$$

$$= q(\frac{\partial\Phi}{\partial t} - \vec{v}\frac{\partial\vec{A}}{\partial t}) \tag{1.47}$$

If one assumes now, that the wake fields are constant during the trapping process, then

$$(\frac{\partial}{\partial t} + v_\phi\frac{\partial}{\partial z})f = f(z - v_\phi t) \tag{1.48}$$

$$(\frac{\partial}{\partial t} + v_\phi\frac{\partial}{\partial z})f = 0 \;\forall\; f(\vec{r}, z - v_\phi t) \tag{1.49}$$

which is especially true for the hamiltonian.

$$\frac{d}{dt}H = q(\frac{\partial\Phi}{\partial t} - \vec{v}\frac{\partial\vec{A}}{\partial t})$$
$$= -qv_\phi(\frac{\partial\Phi}{\partial z} - \vec{v}\frac{\partial\vec{A}}{\partial z})$$

Since $H - v_\phi P_z = \text{const.}$

$$H - v_\phi P_z = \text{const.} \tag{1.50}$$

$$\gamma mc^2 + \Psi - v_\phi p_z - v_\phi q A_z = \text{const.} \tag{1.51}$$

$$\gamma + \frac{q\Phi}{mc^2} - v_\phi\frac{p_z}{mc^2} = \text{const.} \tag{1.52}$$

$$\gamma - v_\phi\frac{p_z}{mc^2} - \underbrace{\frac{q}{mc^2}(\Phi - v_\phi A_z)}_{\bar{\Psi}} = \text{const.} \tag{1.53}$$

$\bar{\Psi}$ is the trapping potential, that determines the potential difference for an electron in a potential that moves with a phase velocity v_ϕ with respect to the laboratory frame. It is valid for small as for relativistic velocities. With the trapping potential one can calculate if an electron inside the plasma wake will be accelerated or not i.e. if electrons will be able to catch up with the wake's velocity during the propagation of the wake or if it will slip out of the potential. From the prior calculations a general formula can be determined, that compares

$$\Delta\bar{\Psi} = \bar{\Psi}_\mathrm{i} - \bar{\Psi}_\mathrm{f} = \gamma_\mathrm{f} - \gamma_\mathrm{i} - \gamma_f\frac{v_\phi v_\mathrm{f}}{c^2} + \gamma_\mathrm{i}\frac{v_\phi v_\mathrm{i}}{c^2} \tag{1.54}$$

In order to honor the name "trapping potential" i.e. to apply this derivation to make predictions of the electron trapping behavior in the plasma wake, it is necessary to define a trapping condition. An obvious and conventional choice is that an electron should catch up with the wake's velocity so that $v_\mathrm{f} = v_\phi$. Equation (1.54) consequently simplifies to

$$\Delta\bar{\Psi} = \gamma_\phi - \gamma_\mathrm{i} - \gamma_\phi \frac{v_\phi^2}{c^2} + \gamma_\mathrm{i} \frac{v_\phi v_\mathrm{i}}{c^2} \tag{1.55}$$

Equation (1.55) can be further separated into different physical cases:

luminal wakefield, electron injected at rest

In this case the plasma wake travels with a phase velocity near the speed of light, which is the case for beam-driven scenarios with high γ driver beams ($v_\phi \approx c$), and electrons starting inside the wake initially at rest ($v_\mathrm{i} \approx 0$). Here Equation (1.55) simplifies to

$$\Delta\bar{\Psi} = -1 \tag{1.56}$$

Examples of this case are the underdense photocathode, or Trojan Horse injection [14], or wakefield induced ionization injection [15].

luminal wakefield, electron injected with $v \neq 0$

In external injection schemes the electrons are already pre-accelerated when they are injected into the wake so that the trapping condition becomes

$$\Delta\bar{\Psi} = -\gamma_\mathrm{i}(1 - \frac{v_\mathrm{i} v_\phi}{c^2}) \approx -\gamma_\mathrm{i}(1 - \frac{v_\mathrm{i}}{c}). \tag{1.57}$$

subluminal wakefield, electron injected at rest

$$\Delta\bar{\Psi} = \gamma_\phi(1 - \frac{v_\phi^2}{c^2}) - 1 = \gamma_\phi^{-1} - 1 \tag{1.58}$$

This formula can for example be applied to ionization injection in LWFA [16] or beam-driven ionization injection schemes in which the wake's phase velocity is retarded such as the Downramp-assisted Trojan Horse (DTH) [17], which this work has as special focus on. In latter case mathematically strictly speaking $\frac{dH}{dt} \neq 0$, but for small changes $\frac{dH}{dt} \approx 0$ during the injection process of the electrons, equation (1.58) can still be applied.

superluminal wakefield

There are physical situations imaginable in which the wake or at least part of the wake move with a phase velocity faster than the speed of light. This is the case for example when a beam driven wake traverses an electron density upramp. From the previous deductions it seems obvious, that trapping electrons in such a superluminal wakefield is not possible, as γ_ϕ^{-1} becomes complex for $v_\phi > c$.

However, if the superluminosity is only transient as with a short density upramp, the phase velocity will return to c right after the transition. In this case trpping can be possible, but the mathematic tool presented in this section is insufficient to describe the trapping and the phase velocity after the transition is setting the demand on the potential.

1.7.1 Trapping position and bunch compression

Assuming that the longitudinal wake field $\frac{\partial E_z}{\partial r} = 0$ for a sufficiently wide radius the trapping behaviour can be seen in 1D only. In the blowout regime the acceleration gradient is to second order linear in ξ (compare section (1.4)) with

$$E_z(\xi) = \tilde{E_0}\xi. \tag{1.59}$$

One should keep in mind that the origin of the coordinate system has been shifted so that $\xi = 0$ is at the zero-crossing of the electric field. $\tilde{E_0}$ is the slope of the accelerating field. This will be filled with values later on, but for now we are just interested in a more general derivation. Additionally equation (1.59) is only valid within the boundaries $[-\lambda_p/2, \lambda_p/2]$. Integrating erquation (1.59) gives the potential

$$U_z(\xi) = \frac{1}{2}\tilde{E_0}\xi^2. \tag{1.60}$$

Now equation (1.60) is inserted in equation (1.56) and rearranged in order to find for an electron released at an inital position ξ_i its trapping position ξ_f by deriving

$$\bar{\Psi}_f - \bar{\Psi}_i = -1 \tag{1.61}$$

$$U_z(\xi_f) - U_z(\xi_i) = -\frac{m_e c^2}{q_e} \tag{1.62}$$

$$(\xi_i^2 - \xi_f^2) = -\underbrace{\frac{2m_e c^2}{\hat{E_0} q_e}}_{\alpha_t} \tag{1.63}$$

$$\xi_f = -\sqrt{\xi_i^2 + \alpha_t}. \tag{1.64}$$

Equation (1.64) is now the relation between release and trapping position of an electron in the co-moving frame for an accelerating field approximated to be linear. Merely negative values are considered, as a trapping only happens at the back of the wake. Forth going with our calculation we would like to handle a distribution of electrons to get closer to the description of the witness electron beam. This finding can than be used to calculate the compression of a released electron beam during the trapping. For that we start with a 1D spatial Gaussian distribution with rms length σ_ξ. We will later see that this assumption in fact resembles very well the distribution of interest.

$$f(\xi) = \frac{1}{\sigma_\xi\sqrt{2\pi}} e^{-\frac{(\xi+\delta_\xi)^2}{2\sigma_\xi^2}}. \tag{1.65}$$

The distribution should be normalized to

$$\int_{-\infty}^{\infty} f(\xi) d\xi \stackrel{!}{=} 1. \tag{1.66}$$

Equation (1.65) is now the initial injected electron beam and can, by applying equation (1.64) be used to calculate the trapped electron beam distribution.

$$f_{\mathrm{f}}(\xi) = f(\xi_{\mathrm{i}}(\xi_{\mathrm{f}}))\| \frac{\partial \xi_{\mathrm{f}}}{\partial \xi_{\mathrm{i}}} \| \tag{1.67}$$

$$= \frac{1}{\sigma_\xi \sqrt{2\pi}} e^{-\frac{(\sqrt{\xi_{\mathrm{f}}^2 - \alpha_{\mathrm{t}}} + \delta_\xi)^2}{2\sigma_\xi^2}} \frac{\xi_{\mathrm{i}}}{\sqrt{\xi_{\mathrm{i}}^2 + \alpha_{\mathrm{t}}}} \tag{1.68}$$

$$= \frac{1}{\sigma_\xi \sqrt{2\pi}} e^{-\frac{(\sqrt{\xi_{\mathrm{f}}^2 - \alpha_{\mathrm{t}}} + \delta_\xi)^2}{2\sigma_\xi^2}} \frac{\sqrt{\xi_{\mathrm{f}}^2 - \alpha_{\mathrm{t}}}}{\sqrt{\sqrt{\xi_{\mathrm{f}}^2 - \alpha_{\mathrm{t}}}^2 + \alpha_{\mathrm{t}}}} \tag{1.69}$$

$$= \frac{1}{\sigma_\xi \sqrt{2\pi}} e^{-\frac{(\sqrt{\xi_{\mathrm{f}}^2 - \alpha_{\mathrm{t}}} + \delta_\xi)^2}{2\sigma_\xi^2}} \frac{\sqrt{\xi_{\mathrm{f}}^2 - \alpha_{\mathrm{t}}}}{\sqrt{\xi_{\mathrm{f}}^2 - \alpha_{\mathrm{t}} + \alpha_{\mathrm{t}}}} \tag{1.70}$$

$$= \frac{1}{\sigma_\xi \sqrt{2\pi}} e^{-\frac{(\sqrt{\xi_{\mathrm{f}}^2 - \alpha_{\mathrm{t}}} + \delta_\xi)^2}{2\sigma_\xi^2}} \frac{\sqrt{\xi_{\mathrm{f}}^2 - \alpha_{\mathrm{t}}}}{\sqrt{\xi_{\mathrm{f}}^2 - \alpha_{\mathrm{t}} + \alpha_{\mathrm{t}}}} \tag{1.71}$$

$$= \frac{1}{\sigma_\xi \sqrt{2\pi}} e^{-\frac{(\sqrt{\xi_{\mathrm{f}}^2 - \alpha_{\mathrm{t}}} + \delta_\xi)^2}{2\sigma_\xi^2}} \frac{\sqrt{\xi_{\mathrm{f}}^2 - \alpha_{\mathrm{t}}}}{\sqrt{\xi_{\mathrm{f}}^2}} \tag{1.72}$$

$$= \frac{1}{\sigma_\xi \sqrt{2\pi}} e^{-\frac{(\sqrt{\xi_{\mathrm{f}}^2 - \alpha_{\mathrm{t}}} + \delta_\xi)^2}{2\sigma_\xi^2}} \frac{\sqrt{\xi_{\mathrm{f}}^2 - \alpha_{\mathrm{t}}}}{\xi_{\mathrm{f}}} \tag{1.73}$$

$$= \frac{1}{\sigma_\xi \sqrt{2\pi}} e^{-\frac{(\sqrt{\xi_{\mathrm{f}}^2 - \alpha_{\mathrm{t}}} + \delta_\xi)^2}{2\sigma_\xi^2}} \sqrt{1 - \frac{\alpha_{\mathrm{t}}}{\xi_{\mathrm{f}}^2}} \tag{1.74}$$

$$\tag{1.75}$$

One should note here, that equation (1.74) as well as equation (1.65) offer positive as well as negative solutions due to the symmetry of the potential. Causality and the physics of accelerators does of course only allow solutions with $\xi_{\mathrm{f}} < 0$. Since we assume that no charge is lost or created during trapping for $f_f(\xi)$ as well a normalization so that

$$\int_{-\infty}^{0} f_f(\xi) d\xi \stackrel{!}{=} 1 \tag{1.76}$$

is required.

Equation (1.74) can be seen a response function to an electron release.

A complete description of velocity bunching as it occurs in wakefields is described in [18, 19].

1.8 Acceleration methods in PWFA

The strong accelerating fields in PWFA can be harvested with a variety of methods. They differ in experimental complexity, demand towards drive beam

1.8.1 External injection - Double bunch

External injection is the least complex PWFA setup and is also the method that has been demonstrated much earlier than other methods. The basic idea is that a plasma wake is set up by an electron beam, electrons - either from the same electron beam or by a trailing electron beam - are accelerated, if they are at the right phase with respect to the wake.

The first experimental realization of a PWFA was established in 1988 at the Argonne advanced accelerator test facility (AATF) [20]. With a method successfully applied to measure the wake fields in accelerating structures a $2-3$ nC electron beam with a rms bunch length of 2.4mm was used to drive a wake in a 33 cm long plasma at a density of the order of 10^{13} cm^{-3}. The driving bunch was trailed by a low-charge witness beam with variable delay to scan the wake fields. The oscillating nature of the wake fields was well measured with a maximum accelerating gradient of 1.6 MeV/m. With a higher driver witness beam charge of 4 nC [21] it was possible to show a non-linear wake with an accelerating gradient of 5.3 MeV/m.

In 2006 at the Final Focus Test Beam Facility (FFTB) at the Stanford Linear Accelerator Center (SLAC) the blow-out regime was finally reached as described in [22]. A 42 GeV electron beam with a spot size of 10 μm and rms bunch length of 15 μm propagated through a 85 cm Li oven. The shorter, high current bunch now allowed for driving a wake in a much higher plasma density of 2.7×10^{17} cm^{-3} in the blowout regime. Thanks to the extremely high wake field gradient of 52 GeV/m which effectively accelerated part of the electron beam to up to 85 GeV.

The successor experiment to the plasma experiments at the FFTB is the Facility for Advanced Accelerator Experimental Tests (FACET) [23]. Several double-bunch experiments have been successfully conducted. At FACET the double-bunches are produced by accelerating one long electron bunch all the way to the final chicane. While the chirped bunch is dispersed, the central part is cut out by a mask which results in a scrape in the current profile [24]. This method has the advantage that the transport of the beam along the LINAC is only required for one bunch. Efficiency and beamloading effects were studied in [25] and recently at FACET a double-bunch acceleration of positrons in a positron-driven wake was demonstrated by shaping the transverse plasma shape to a hollow channel, which effectively avoids any transverse fields that would otherwise defocus the positrons [26].

1.8.2 Density Downramp injection

1.8.3 Plasma Torch

[27, 28]

1.8.4 ionization injection

In all previously outlined injection types, electrons to be accelerated in the wake are at a nonzero velocity when injected, which is an advantage as regards the requirements on the wakefield gradient. Ionization injected electrons are in a bound state until they are released to continuum inside the wake. This from a physics standpoint requires the plasma to only be partially ionized when the wake is excited and from an engineering stand point ionization levels that are sufficiently distinct in their ionization rates to ensure a controlled ionization. We will further use the term Low ionization threshold (LIT) medium for the part to be ionized in order to drive the wave in it and High ionization threshold (HIT) medium for the part that originates the injected witness beam electrons. Of course, HIT and LIT medium can be the same, by making use of different ionization levels. If, however,

HIT and LIT are different gases as e.g. H_2 and He, their gas density ratio becomes a handy degree of freedom to control the injected charge. Experimentally in [29] ionization ionjection was shown in a Rb oven. The electron beam head electric fields were used to ionize $Rb \rightarrow Rb^+$, while the drive beam tails' field overlapped with the wake electric fields were strong enough to ionize $Rb^+ \rightarrow Rb^{2+}$ and inject the. This method of injection electrons is conceptually comparable to ionization injection, where the driving laser pulse fields are strong enough to ionize several ionization levels with injection at the back of the laser or in other words the front of the wake [30].

In [31] and [15] with theory and simulations a setup was examined where only the back of the wake had sufficiently high fields to ionize the HIT medium and combined with the concept of the trapping potential as described in section (1.7). It could be shown that the combined requirements for trapping, i.e. the overlap of the ionization region and the trapping region, confine the possible electron source which enables the generation of low emittance electron beams ($\epsilon_x = 1.5\ \mu$m)

1.8.5 Trojan Horse injection

The underdense photocathode or Trojan Horse injection is one of the most complex injection techniques. It was proposed by B. Hidding in [14]. Neither the wake nor the beam electric fields are sufficient to ionize the HIT medium. Instead this is the duty of an additional short-pulse laser pulse, trailing the driving electron beam. Given full control over laser-to-electron beam alignment and synchronization, it is possible to ionize and release electrons wherever in the wake it deems necessary. It could be shown that a release in the potential minimum, i.e. the zero-crossing of the wake is particularly advantageous, because the electron acceleration to relativistic speed is extremely rapid ($\approx \frac{\lambda_p}{2c}$) and the bunch compression is maximum at this injection position. Furthermore the emittance of Trojan Horse injected electron beams can be very low on the order of a few $\epsilon_{\mathrm{rms}} \approx 10^{-8}$ mrad. The reasons for that lie to one part in the ionization method. A typical 800 nm Ti:Sa few fs laserpulse only needs a peak intensity of 10^{15} W/cm^2 to ionize a HIT medium as e.g. $He \rightarrow He^+$. The normalized vector potential $a_0 = \frac{q_e E_0}{m_e c^2} = 0.022 << 1$ implies that no ponderomotive force can be expected that would impose an inital transverse momentum to the released electron bunch wo that the transverse momentum is basically determined by the HIT gas temperature. A detailed theoretically supported PIC simulation parameter scan in [32] examined scalings between witness emittance and brightness and laser beam parameters as beam waist w_0, pulse length and peak intensity. A indifference towards pulse length as well as an emittance increase with w_0 and intensity could be demonstrated.

In [33] a detailed comparison between laser and electron beam driven wakefield acceleration is drawn out.

1.9 Trapping behaviour for the Trojan Horse Injection

1.9.1 The role of the ionization front

We saw in section (1.7.1) that the length and position of the originally released electron bunch as well as the accelerating gradient plays a significant role for establishing an effective velocity bunching. In the Trojan Horse injection concept it is possible to inject electrons at a phase of choice. We want to examine now what kind of initial electron bunch distributions we can expect. For that we start with a 1D consideration. We combine this with the information from section (1.1.2) and will

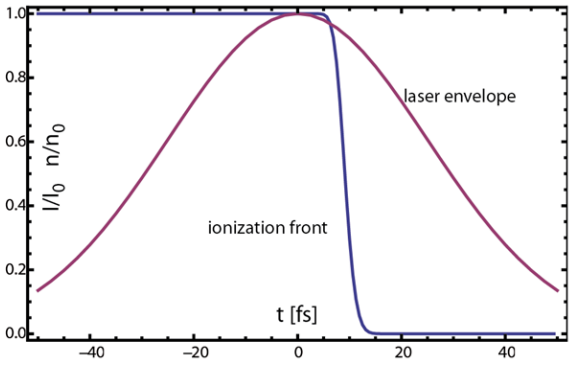

Fig. 1.3: Ionization front from a

Figure (1.3) demonstrates the time-dependent ionization ratio in He during the propagation of a ??? fs long laser pulse with peak intensity ??? , according to equation (1.27). The ionization front is clearly visible as a rapid increase of the ionization ratio. In Kim-ionfront-paper it has been shown experimentally that the ADK formalism is in fact reliable as regards the prediction of the ionization front. From that we can calculate the inital electron release distribution

$$f_{\mathrm{i}}(\xi) = \frac{d}{dt} n_0 \Big(1 - \exp\Big(-\int_{-\infty}^{t} W_{\mathrm{ADK}}(E_x(r,z,t'))dt'\Big)\Big) \tag{1.77}$$

$$= n_0 \frac{d}{dt} \exp\Big(-\int_{-\infty}^{t} W_{\mathrm{ADK}}(E_x(r,z,t'))dt'\Big). \tag{1.78}$$

Two things are important to notice:

1. The ionization front and with that the initial release is much shorter than the actual laser pulse.

2. The center of the release electron distribution does not need to coincide with the center of the laser pulse.

We now want to further investigate on the initial electron release distribution ans how it depends on laser peak intensity and pulse lengths.

1.9.2 Dark current mitigation

Simulation

[34]

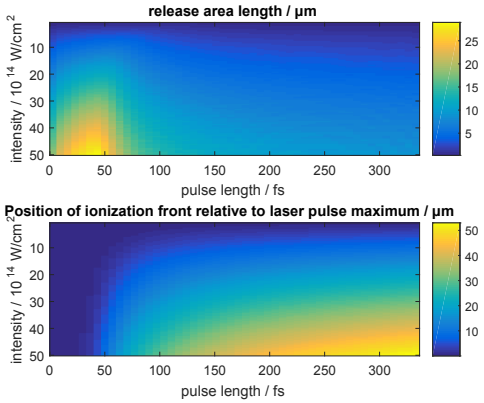

Experiment

1.9.3 Downramp assisted Trojan Horse

1.10 numerical modeling of Trojan Horse injection

1.10.1 emittance growth from space charge

1.10.2 Laser parameter variations

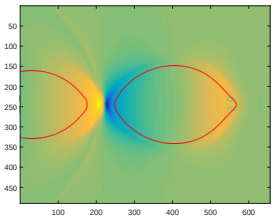
50
100
150
200
250
300
350
400
450
100
200
300
400
500
600

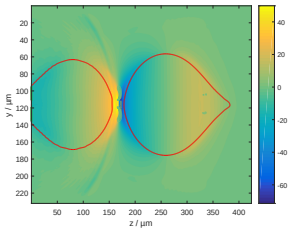
20
40
60
80
100
120
140
160
180
200
220
y / µm
50
100
150
200
250
300
350
400
z / µm
40
20
0
-20
-40
-60

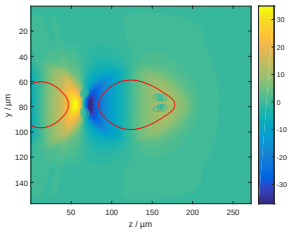
20
40
60
80
100
120
140
y / µm
50
100
150
200
250
z / µm
30
20
10
0
-10
-20
-30

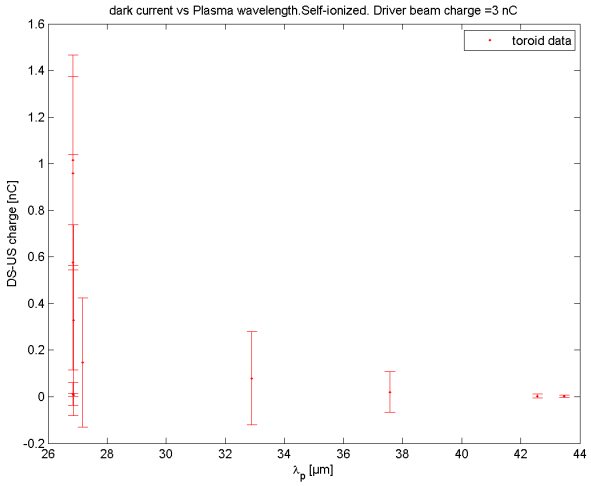

Fig. 1.4: Experimental evidence of dark current reduction in beam-ionized plasma

2. EXPERIMENT

BIBLIOGRAPHY

[1] Francsis F. Chen. *Introduction to Plasma Physics and Controlled Fusion*, volume 1. Plenum Press New York and London, 1974.

[2] Peter Mulser and Dieter Bauer. *High power laser-matter interaction*, volume 238. Springer Science & Business Media, 2010.

[3] MV Ammosov, NB Delone, VP Krainov, AM Perelomov, VS Popov, MV Terent'ev, Gennady L Yudin, and Misha Yu Ivanov. Tunnel ionization of complex atoms and of atomic ions in an alternating electric field. *Sov. Phys.JETP*, 64, 1986.

[4] David L Bruhwiler, DA Dimitrov, John R Cary, Eric Esarey, Wim Leemans, and Rodolfo E Giacone. Particle-in-cell simulations of tunneling ionization effects in plasma-based accelerators. *Physics of Plasmas (1994-present)*, 10(5):2022–2030, 2003.

[5] R.L. Kelly. *Atomic and ionic spectrum lines below 2000A: hydrogen through argon.* Oct 1982.

[6] E. Esarey, C. B. Schroeder, and W. P. Leemans. Physics of laser-driven plasma-based electron accelerators. *Rev. Mod. Phys.*, 81:1229–1285, Aug 2009.

[7] Pisin Chen, J. J. Su, J. M. Dawson, K. L. F. Bane, and P. B. Wilson. Energy transfer in the plasma wake-field accelerator. *Phys. Rev. Lett.*, 56:1252–1255, Mar 1986.

[8] KL Bane, Perry B Wilson, and T Weiland. Wake fields and wake field acceleration. In *AIP Conf. Proc.*, volume 127, pages 875–928, 1984.

[9] W. K. H. Panofsky and W. A. Wenzel. Some considerations concerning the transverse deflection of charged particles in radio-frequency fields. *Review of Scientific Instruments*, 27(11):967–967, 1956.

[10] Helmut Wiedemann. *Particle Accelerator Physics*, volume 3. Springer-Verlag, 2007.

[11] J. B. Rosenzweig. *Fundamentals of Beam Physics.* Oxford: Oxford University Press, 2003.

[12] E.D Courant and H.S Snyder. Theory of the alternating-gradient synchrotron. *Annals of Physics*, 3(1):1 – 48, 1958.

[13] Klaus Floettmann. Some basic features of the beam emittance. *Phys. Rev. ST Accel. Beams*, 6:034202, Mar 2003.

[14] B. Hidding, G. Pretzler, J. B. Rosenzweig, T. Königstein, D. Schiller, and D. L. Bruhwiler. Ultracold electron bunch generation via plasma photocathode emission and acceleration in a beam-driven plasma blowout. *Phys. Rev. Lett.*, 108:035001, Jan 2012.

[15] A. Martinez de la Ossa, C. Behrens, J. Grebenyuk, T. Mehrling, L. Schaper, and J. Osterhoff. High-quality electron beams from field-induced ionization injection in the strong blow-out regime of beam-driven plasma accelerators. *Nuclear Instruments and Methods in Physics Research Section A: Accelerators, Spectrometers, Detectors and Associated Equipment*, 740:231 – 235, 2014. Proceedings of the first European Advanced Accelerator Concepts Workshop 2013.

[16] A. Pak, K. A. Marsh, S. F. Martins, W. Lu, W. B. Mori, and C. Joshi. Injection and trapping of tunnel-ionized electrons into laser-produced wakes. *Phys. Rev. Lett.*, 104:025003, Jan 2010.

[17] Georg Wittig Henning Groth Yunfeng Xi Aihua Deng James Benjamin Rosenzweig David Leslie Bruhwiler Johnathan Smith Dino Anthony Jaroszynski Zheng-Ming Sheng Grace Gloria Manahan Guoxing Xia Steven Jamison Bernhard Hidding Alexander Knetsch, Oliver Karger. Downramp-assisted underdense photocathode electron bunch generation in plasma wakefield accelerators. *Physical Review Letters*, 2016.

[18] S. G. Anderson, P. Musumeci, J. B. Rosenzweig, W. J. Brown, R. J. England, M. Ferrario, J. S. Jacob, M. C. Thompson, G. Travish, A. M. Tremaine, and R. Yoder. Velocity bunching of high-brightness electron beams. *Phys. Rev. ST Accel. Beams*, 8:014401, Jan 2005.

[19] L Serafini and M Ferrario. Velocity bunching in photo-injectors. In *AIP conference proceedings*, pages 87–106. IOP INSTITUTE OF PHYSICS PUBLISHING LTD, 2001.

[20] James Benjamine Rosenzweig, DB Cline, B Cole, H Figueroa, W Gai, R Konecny, J Norem, P Schoessow, and J Simpson. Experimental observation of plasma wake-field acceleration. *Physical review letters*, 61(1):98, 1988.

[21] H Figueroa, W Gai, R Konecny, J Norem, A Ruggiero, P Schoessow, and J Simpson. Direct measurement of beam-induced fields in accelerating structures. *Physical review letters*, 60(21):2144, 1988.

[22] Ian Blumenfeld, Christopher E Clayton, Franz-Josef Decker, Mark J Hogan, Chengkun Huang, Rasmus Ischebeck, Richard Iverson, Chandrashekhar Joshi, Thomas Katsouleas, Neil Kirby, et al. Energy doubling of 42 gev electrons in a metre-scale plasma wakefield accelerator. *Nature*, 445(7129):741–744, 2007.

[23] CI Clarke, FJ Decker, RJ England, R Erikson, C Hast, MJ Hogan, SZ Li, M Litos, Y Nosochkov, J Seeman, et al. Facet: Slacs new user facility. *Energy [GeV]*, 23:20, 2012.

[24] MJ Hogan, TO Raubenheimer, A Seryi, P Muggli, T Katsouleas, C Huang, W Lu, W An, KA Marsh, WB Mori, et al. Plasma wakefield acceleration experiments at facet. *New Journal of Physics*, 12(5):055030, 2010.

[25] M Litos, E Adli, W An, CI Clarke, CE Clayton, Sébastien Corde, JP Delahaye, RJ England, AS Fisher, J Frederico, et al. High-efficiency acceleration of an electron beam in a plasma wakefield accelerator. *Nature*, 515(7525):92–95, 2014.

[26] Spencer Gessner. *Demonstration of the Hollow channel Plasma WakefWake Accelerator*. PhD thesis, Stanford University, 2016.

[27] G Wittig, O Karger, A Knetsch, Y Xi, A Deng, JB Rosenzweig, DL Bruhwiler, J Smith, GG Manahan, Z-M Sheng, et al. Optical plasma torch electron bunch generation in plasma wakefield accelerators. *Physical Review Special Topics-Accelerators and Beams*, 18(8):081304, 2015.

[28] Georg Wittig, Oliver S Karger, Alexander Knetsch, Yunfeng Xi, Aihua Deng, James B Rosenzweig, David L Bruhwiler, Jonathan Smith, Zheng-Ming Sheng, Dino A Jaroszynski, et al. Electron beam manipulation, injection and acceleration in plasma wakefield accelerators by optically generated plasma density spikes. *Nuclear Instruments and Methods in Physics Research Section A: Accelerators, Spectrometers, Detectors and Associated Equipment*, 2016.

[29] N. Vafaei-Najafabadi, K. A. Marsh, C. E. Clayton, W. An, W. B. Mori, C. Joshi, W. Lu, E. Adli, S. Corde, M. Litos, S. Li, S. Gessner, J. Frederico, A. S. Fisher, Z. Wu, D. Walz, R. J. England, J. P. Delahaye, C. I. Clarke, M. J. Hogan, and P. Muggli. Beam loading by distributed injection of electrons in a plasma wakefield accelerator. *Phys. Rev. Lett.*, 112:025001, Jan 2014.

[30] A. Pak, K. A. Marsh, S. F. Martins, W. Lu, W. B. Mori, and C. Joshi. Injection and trapping of tunnel-ionized electrons into laser-produced wakes. *Phys. Rev. Lett.*, 104:025003, Jan 2010.

[31] A. Martinez de la Ossa, J. Grebenyuk, T. Mehrling, L. Schaper, and J. Osterhoff. High-quality electron beams from beam-driven plasma accelerators by wakefield-induced ionization injection. *Phys. Rev. Lett.*, 111:245003, Dec 2013.

[32] Y Xi, B Hidding, D Bruhwiler, G Pretzler, and JB Rosenzweig. Hybrid modeling of relativistic underdense plasma photocathode injectors. *Physical Review Special Topics-Accelerators and Beams*, 16(3):031303, 2013.

[33] B Hidding, GG Manahan, O Karger, A Knetsch, G Wittig, DA Jaroszynski, ZM Sheng, Y Xi, A Deng, JB Rosenzweig, et al. Ultrahigh brightness bunches from hybrid plasma accelerators as drivers of 5th generation light sources. *Journal of Physics B: Atomic, Molecular and Optical Physics*, 47(23):234010, 2014.

[34] G. G. Manahan, A. Deng, O. Karger, Y. Xi, A. Knetsch, M. Litos, G. Wittig, T. Heinemann, J. Smith, Z. M. Sheng, D. A. Jaroszynski, G. Andonian, D. L. Bruhwiler, J. B. Rosenzweig, and B. Hidding. Hot spots and dark current in advanced plasma wakefield accelerators. *Phys. Rev. Accel. Beams*, 19:011303, Jan 2016.

[35] S Z Green, E Adli, C I Clarke, S Corde, S A Edstrom, A S Fisher, J Frederico, J C Frisch, S Gessner, S Gilevich, P Hering, M J Hogan, R K Jobe, M Litos, J E May, D R Walz, V Yakimenko, C E Clayton, C Joshi, K A Marsh, N Vafaei-Najafabadi, and P Muggli. Laser ionized preformed plasma at facet. *Plasma Physics and Controlled Fusion*, 56(8):084011, 2014.

[36] Allied Vision, https://www.alliedvision.com/en/products/cameras/detail/Manta/G-125.html. *Manta G-125 Data sheet.*

[37] X. Yan, A. M. MacLeod, W. A. Gillespie, G. M. H. Knippels, D. Oepts, A. F. G. van der Meer, and W. Seidel. Subpicosecond electro-optic measurement of relativistic electron pulses. *Phys. Rev. Lett.*, 85:3404–3407, Oct 2000.

[38] Bernd Richard Steffen. *Electro-Optic Methods for Longitudinal Bunch Diagnostics at FLASH.* PhD thesis, University of Hamburg, 2007.